

Artificial Neural Network as a FPGA Trigger for a Detection of Very Inclined Air Showers

Zbigniew Szadkowski, *Member, IEEE*, K. Pytel

Abstract—The observation of ultra-high energy neutrinos (UHE ν s) has become a priority in experimental astroparticle physics. Neutrinos can interact in the atmosphere (downward-going ν) or in the Earth crust (Earth-skimming ν), producing air showers that can be observed with arrays of detectors at the ground. The surface detector array of the Pierre Auger Observatory can detect these types of cascades. The distinguishing signature for neutrino events is the presence of very inclined showers produced close to the ground (i.e., after having traversed a large amount of atmosphere). Up to now, the Pierre Auger Observatory did not find any candidate for a neutrino event. This imposes competitive limits to the diffuse flux of UHE ν s.

A very low rate of events potentially generated by neutrinos is a significant challenge for a detection technique and requires both sophisticated algorithms and high-resolution hardware. We present a trigger based on a pipeline artificial neural network implemented in a large FPGA which after learning can recognize traces corresponding to special types of events.

The structure of an artificial neural network algorithm being developed on the MATLAB platform has been implemented into the fast logic of the biggest Cyclone[®] V E FPGA used for the prototype of the Front-End Board for the Auger-Beyond-2015 effort. Several algorithms were tested, however, the Levenberg-Marquardt one (trainlm) seems to be the most efficient.

The network was taught: a) to recognize "old" showers (learning on a basis of real very inclined Auger showers (positive markers) and real standard showers especially triggered by Time over Threshold (negative marker), b) to recognize "young" showers (on the basis of simulated "young" events (positive markers) and standard Auger events as a negative reference). A three-layer neural network being taught by real very inclined Auger showers shows a good efficiency in pattern recognition of 16-point traces with profiles characteristic of "old" showers.

Nevertheless, preliminary simulations of showers with the CORSIKA shower simulation package and the response of the water Cherenkov tanks with the OffLine data analyses and reconstruction package suggest that for neutrino showers starting a development deep in the atmosphere, and for relatively low initial energy $\sim 10^{18}$ eV, ADC traces are not too long, and a 16-point analysis should be sufficient for a recognition of "young" showers. The neural network algorithm can significantly support a detection for low energies, where a more intense neutrino stream is expected. For higher energies traces are longer, however, a detector response is strong enough for the showers to be detected by standard amplitude-based triggers.

Index Terms—Pierre Auger Observatory, trigger, FPGA, DCT, neural network.

Manuscript received June 27, 2014. This work was supported by the Polish National Center for Research and Development under NCBiR Grant No. ERA/NET/ASPERA/02/11 and by the National Science Centre (Poland) under NCN Grant No. 2013/08/M/ST9/00322

Zbigniew Szadkowski is with the University of Łódź, Department of Physics and Applied Informatics, Faculty of High-Energy Astrophysics, 90-236 Łódź, Pomorska 149, Poland, (e-mail: zszadkow@kfd2.phys.uni.lodz.pl, phone: +48 42 635 56 59).

Krzysztof Pytel is with the University of Łódź, Department of Physics and Applied Informatics, Faculty of Informatics, 90-236 Łódź, Poland,

I. INTRODUCTION

ULTRA -high energy cosmic ray (UHECR) experiments in energy range of $10^{18} - 10^{20}$ eV are the inspiration for active development of theoretical astrophysics hypotheses [1]. The origin of the UHECRs, their production mechanism and composition still remain a mystery, as do hypothetical fluxes of ultrahigh energy neutrinos (UHE ν s) [2].

Generally, we can classify astrophysical models as: "bottom-up" and "top-down". In the first case, protons and nuclei are accelerated in astrophysical shocks, while pions are produced by cosmic ray interactions with matter or radiation at the source [3]. The second scenario postulates that protons and neutrons are produced from quark and gluon fragmentation of very heavy particles, according to Grand Unified Theories or Super-symmetries, with a supremacy of pions over nucleons [4]. However, "top-down" models have been rather disfavored by the Pierre Auger Observatory due to relatively low photon limits [5]. Protons and nuclei also produce pions due to the Greisen-Zatsepin-Kuzmin (GZK) cutoff [6][7] seen by HiRes [8] and confirmed by the Pierre Auger Observatory [9] [10].

For primary protons, decays of charged pions (as results of photo-pion production associated with the GZK effect) are expected to be the source of ultra-high energy neutrinos (UHE ν s). However, their fluxes are still doubtful. If the primaries are heavy nuclei, the UHE ν s should be significantly suppressed [11].

The observation of UHE ν s should support an explanation of the origin of UHECRs [12]. Neutrinos indicate directly the source of their production due to the absence of any deflection in magnetic fields. Unlike photons, their unimpeded travel from the sources to the Earth may support a confirmation or rejection of production models. UHE ν s can be detected with arrays of detectors at ground level that are currently being used to measure extensive showers produced by cosmic rays, e.g. the Pierre Auger Observatory [13]. The main challenge in this technique is the extraction of showers initiated by neutrinos from the "background" induced by regular cosmic rays.

Neutrinos have very small cross-sections. This implies a very low probability of interaction for any relatively thin target such as at small zenith angles of neutrino incidence, corresponding to a slant depth at the level of 1 kg/cm^2 . Neutrinos can interact at any point along their trajectories. For a very inclined shower the slant depth increases to $\sim 31 \text{ kg/cm}^2$ and neutrino interactions become more probable [14]. Protons, nuclei, or photons usually interact shortly after entering the atmosphere. For inclined showers they produce a narrow muonic pancake (only the muonic component survives), while for

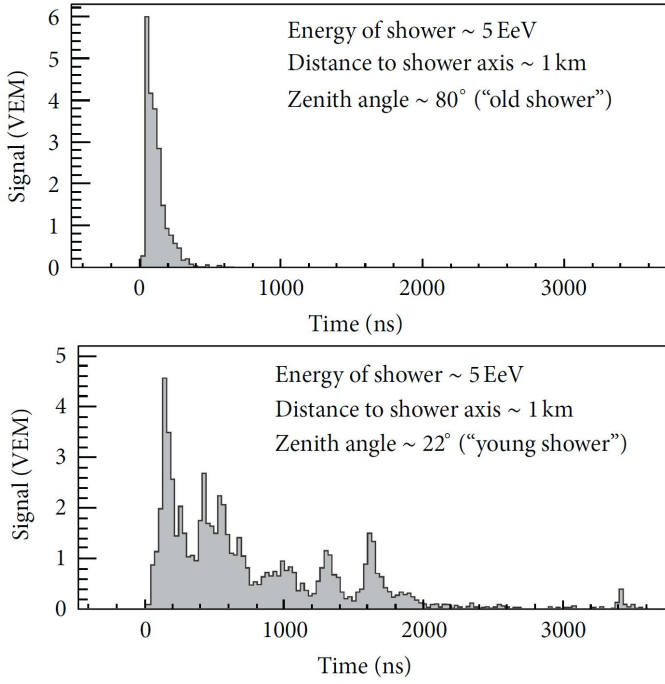


Fig. 1. Simulated ADC traces of stations at 1 km from the shower core for two real showers of 5 EeV. (a) Old extensive air shower ($\theta \sim 80^\circ$). (b) Shower arriving in the early stages of development (young shower) [15].

deeply interacting neutrinos the inclined showers contain also a significant electromagnetic contribution. Inclined showers that interact deep in the atmosphere may be a signature of neutrino events. The surface detector array (SD) of the Pierre Auger Observatory can detect both Earth-skimming and down-going showers [15]. The Earth skimming neutrino events are limited to a very narrow zenith range where the expected background of nucleonic showers is very small. For downward-going neutrino showers there is in principle a larger range of possible zenith angles, but with larger background contamination. This imposes specific algorithms allowing a separation of neutrino-induced showers from nucleonic ones.

In the downward-going channel neutrinos can be generated via both charged and neutral current interactions. Neutrinos of any flavor can induce extensive air showers along the entire path of their development in the atmosphere, also very close to the ground [16].

In the Earth-skimming channel showers can be induced by ν_τ being a product of a τ lepton decaying after the propagation and interaction of an upward-going ν_τ inside the Earth [17].

The surface detector of the Pierre Auger Observatory has good potential to identify and to separate neutrino-induced showers (for both the Earth-skimming and downward-going channels) from showers induced by regular cosmic rays for a large zenith angle ($\theta \geq 70^\circ$). One of the fundamental criteria allowing an identification of neutrino-induced showers is the timing of shower fronts directly observed as profiles of registered traces in the surface detectors.

II. ADC TRACES ANALYSIS

The surface detector array of the Pierre Auger Observatory is able to detect and identify UHE ν s for $E \geq 10^{18}$ eV

[18]. Due to a much larger first interaction cross-section for protons, heavier nuclei and even photons than for neutrinos, their showers usually appear shortly after entering the atmosphere. However, neutrinos can generate showers deeply into the atmosphere. Vertical showers initiated by protons or heavy nuclei have a considerable amount of electromagnetic component at the ground ("young" shower front). However, at high zenith angles ($\theta \geq 70^\circ$) (thicker than about three vertical atmospheres), UHECRs interacting high in the atmosphere generate shower fronts dominated by muons at the ground (an "old" shower front), which generate narrow signals (short ADC traces) spreading over typically tens of nano-seconds in practically all the stations of the event. These traces can be recognized with an algorithm of a 16-point discrete cosine transform (DCT) as well as with a 16-point input artificial neural network (ANN).

For a recognition of the very inclined "old" showers the DCT algorithm [19] was developed and tested on the SD test detector in Malargüe (Argentina) [20] [21]. The algorithm precisely recognized ADC traces of required shapes. Up to now it was tuned for "old" showers, however, it could be optimized also for shapes characteristic for "young" showers. The ANN algorithm is an alternative approach. The efficiency of both algorithms will be tested for both types of showers.

"Young" showers are spread in time over thousands of nano-seconds (Fig. 1) [15]. For the "old" showers practically only the muonic component survives. It gives a short bump in the SD. The "young" showers comprise also some electromagnetic component, which spread the ADC traces in time. However, the muonic component of "young" showers is ahead of the electromagnetic one and gives an early bump. The rising edge of the bump is not so sharp as for the "old" ones, but this signal is also relatively rapidly attenuated, until the electromagnetic component starts to provide its own contribution. The ANN approach can focus on the early bump, to select traces potentially generated by neutrinos.

On the other hand, independent simulations of showers in CORSIKA [22] and a calculation of a response of water Cherenkov detectors (WCDs) in OffLine [23] showed that for neutrino showers (initiated either by ν_μ or ν_τ) for relatively large zenith angle (e.g. 70°) and low altitude (9 km) (to be treated as "young" showers before the maximum of development) there are relatively short ADC traces which can be analyzed also by 16-point pattern engines.

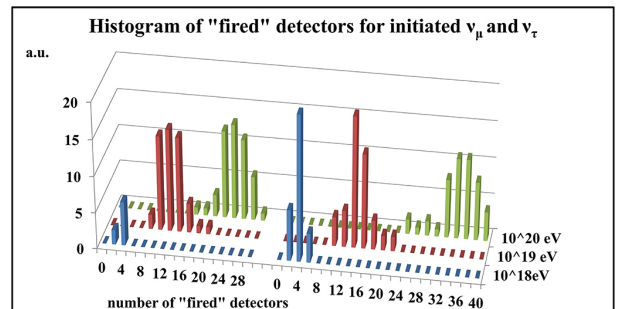


Fig. 2. Histogram of "fired" surface detectors for showers initiated by ν_μ (left panel) and ν_τ (right panel) neutrinos at an altitude of 9350 m.

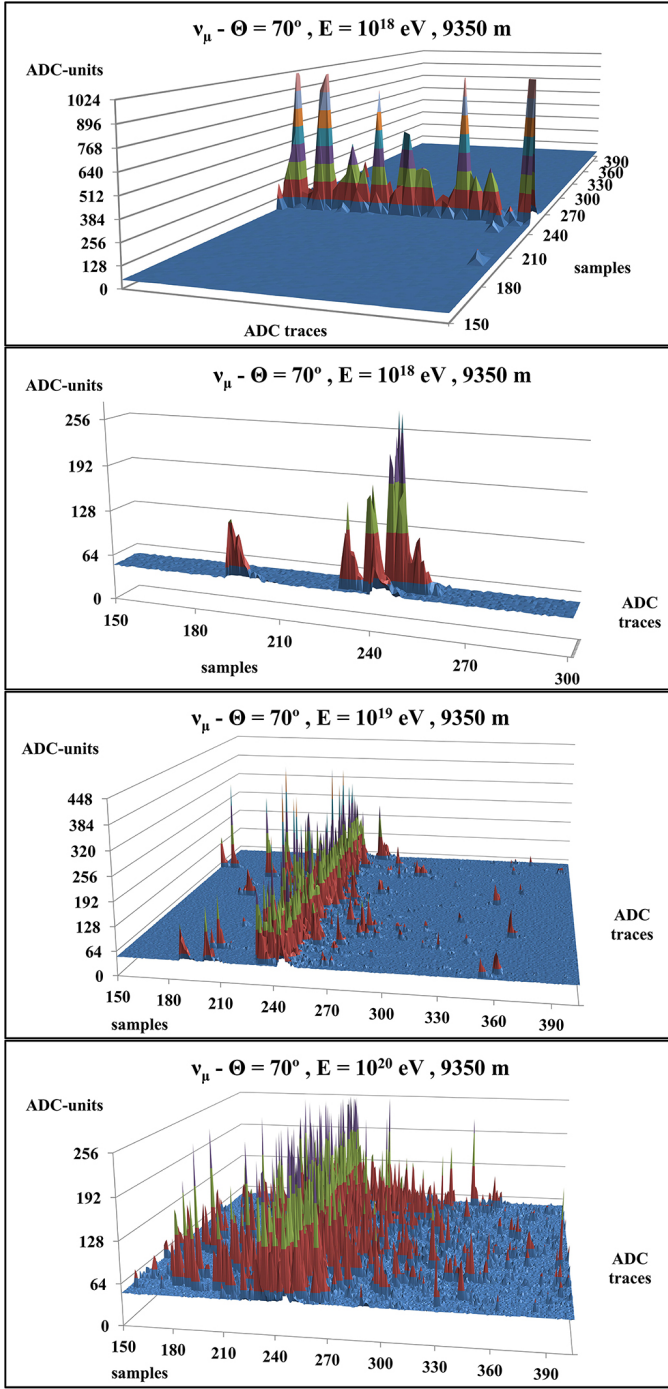


Fig. 3. Simulated ADC traces for 10^{18} , 10^{19} and 10^{20} eV, respectively, for an incident ν_μ at 9350 m and 70° zenith angle. Shown here are events not giving strong enough signals to be detected by a standard trigger.

Showers induced by relatively low-energy neutrinos (in the range of 10^{18} eV) (independently of flavor) can "fire" only a few surface detectors (Fig. 2). These showers may be ignored due to the Auger T3 trigger [24], although they can generate even saturated traces in a few surface detectors (Fig. 5).

Table I shows a fractional rate of simulated events giving 3-fold coincidences on the T1 threshold trigger [24]. For low energy neutrino showers a parallel trigger based on a pattern recognition (i.e. using an artificial neural network) can improve

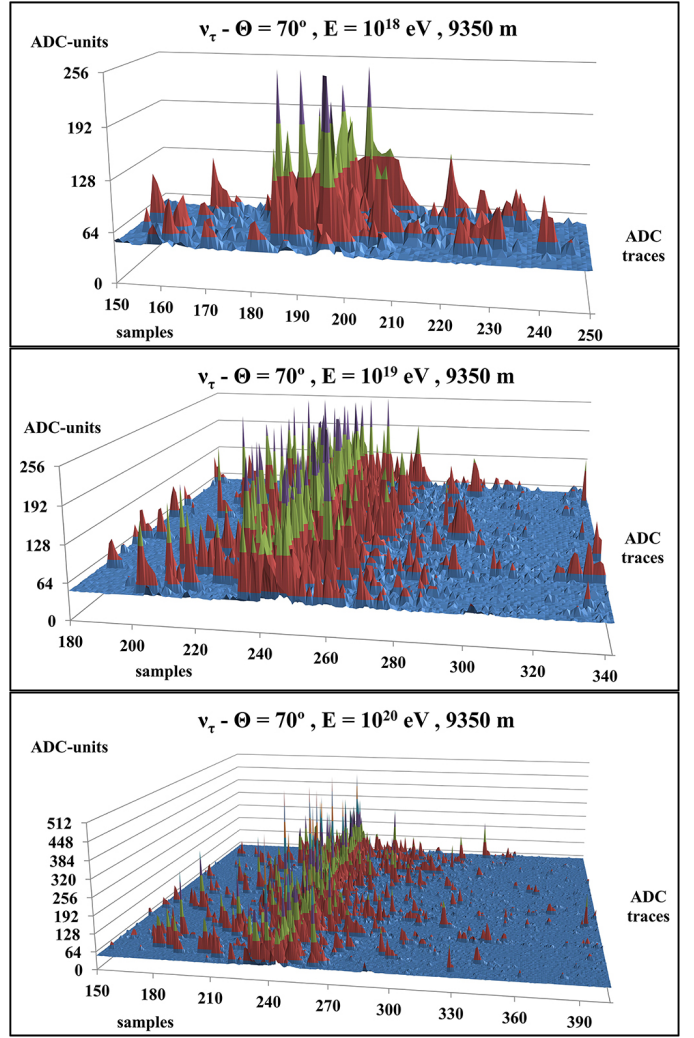


Fig. 4. Simulated ADC traces for 10^{18} , 10^{19} and 10^{20} eV, respectively, for an incident ν_τ at 9350 m and 70° zenith angle. Shown are events with signals too low to be detected by a standard trigger.

the probability of neutrino-induced shower detection.

Figs. 3 and 4 show that ignored events (which do not obey a condition of the T1 threshold trigger), especially for low energies, can be analyzed by the 16-point only algorithm, either the DCT or the ANN one.

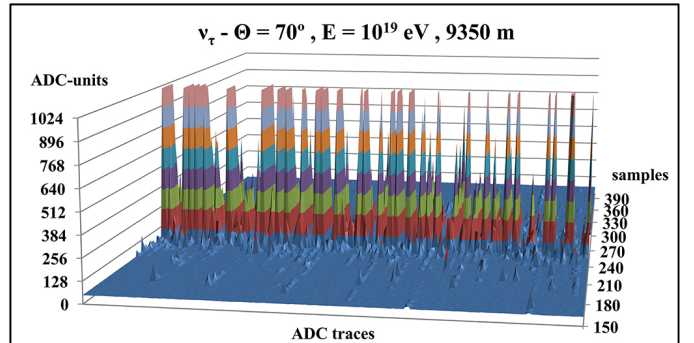


Fig. 5. Simulated ADC traces for incident ν_τ , for energy = 10^{19} eV at 9350 m and 70° zenith angle.

TABLE I
PERCENTAGE OF SIMULATED EVENTS WITH TRACES DETECTED BY
3-FOLD COINCIDENCES (A STANDARD THRESHOLD TRIGGER IN A TIME
DOMAIN)

Energy	ν_μ $\theta = 22^\circ$	ν_τ $\theta = 22^\circ$	ν_μ $\theta = 70^\circ$	ν_τ $\theta = 70^\circ$
10^{18} eV	33 %	10 %	83 %	75 %
10^{19} eV	53 %	40 %	89 %	88 %
10^{20} eV	80 %	83 %	87 %	88 %

III. MATLAB ANALYSIS

The main motivation of an ANN implementation as a shower trigger is the fact that up to now the entire array did not register any neutrino-induced event. The probable reasons are: a) a very low flux of neutrinos and b) amplitudes of ADC-traces that are small and probably below the threshold of the standard 3-fold coincidence trigger. The main idea is to use the ANN approach as a pattern recognition technique.

Several networks were tested (Fig. 6) to get a reasonable compromise between the efficiency of the pattern recognition and a resource occupancy in the FPGA. To train the network we created a database of real Auger inclined "old" showers (as positive marker) and "typical expected neutrino-like signal" (mostly vertical as negative markers). Table II shows results for various teaching configurations used for two networks. Only the Levenberg-Marquardt (Trainlm in MATLAB) algorithm was very efficient. The others showed unacceptable levels of error rates (Table II).

Theoretically, a more complicated network could provide a higher efficiency (Table III), however, it requires much more FPGA resources, especially DSP embedded multipliers. The biggest FPGA from the Cyclone[®] V E family - 5CEFA9F31I7 contains 342 fast DSP embedded multipliers. For 3 independent ANN (for 3 PMTs in the Auger surface detector) we can use 114 DSP blocks per channel. A single neuron (with sixteen 14-bit inputs and 14-bit coefficients) implemented with Altera[®] Multiply Adder v13.1 and PARALLEL_ADD Megafunctions requires 8 DSP blocks (Fig. 8). 114 DSP blocks allow an implementation of 14 neurons per PMT.

The database for training was built from real Auger ADC traces triggered by either Threshold trigger (T1 - 3-fold coincidences for a single time bin for simultaneous signals above 1.75 VEM) or by ToT trigger (at least 13 sub-triggers

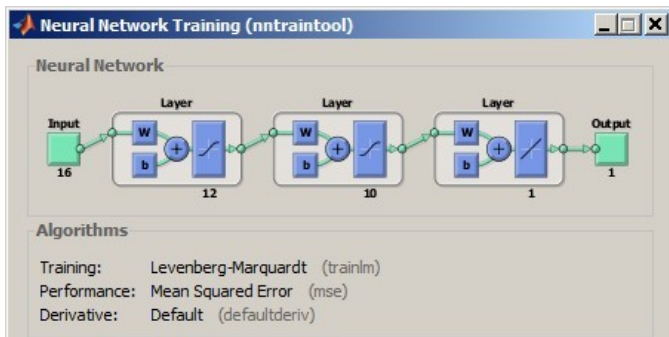


Fig. 6. An example of the ANN structure used for an optimization in Neural Network Training of the MATLAB toolbox.

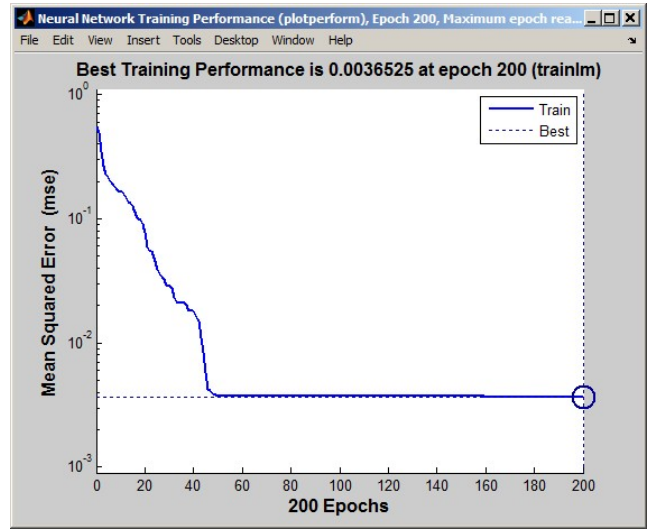


Fig. 7. Training performance for the 3-layer network 12-10-1.

of any 2-fold coincidences in 120 μ s interval, for signals 0.2 VEM above pedestal) [24]. Signals detected by the T1 are relatively strong. The fact that the Pierre Auger Observatory did not register up to now any event potentially generated by a neutrino suggests that the thresholds for standard triggers may be too high. So, we need to teach the network to recognize patterns with much lower amplitudes. We extended the database artificially by reducing the amplitude of real ADC traces (by factors 0.67, 0.5 and 0.25, respectively), keeping the same pedestals and shapes. Table III shows that all networks recognize traces with reduced amplitude pretty well.

The 12-10-1 network offers the best performance with a minimal resource occupancy (Fig. 7, however it requires 23 neurons.

TABLE II
ERROR RATES FOR VARIOUS TRAINING METHODS

ANN	cfg	Traincgp	Traingd	Trainlm	Trainscg
16-12-6-1	Total	27.9 %	42.5 %	0 %	30.7 %
	100 %	27.1 %	41.5 %	0 %	28.7 %
	67 %	24.7 %	41.8 %	0 %	28.4 %
	50 %	28.1 %	42.1 %	0 %	30.6 %
	25 %	31.5 %	44.7 %	0 %	35.0 %
16-12-1	Total	28.7 %	42.0 %	0 %	31.7 %
	100 %	25.9 %	42.8 %	0 %	30.0 %
	67 %	24.7 %	42.5 %	0 %	30.6 %
	50 %	28.1 %	41.5 %	0 %	31.8 %
	25 %	36.2 %	41.2 %	0 %	34.3 %

TABLE III
ERROR RATES FOR 3-LAYER NETWORKS WITH TRAINLM ALGORITHM

ANN	Total	100 %	67 %	50 %	25 %
16-12-1	0.0 %	0.0 %	0.0 %	0.0 %	0.0 %
14-12-1	0.0 %	0.0 %	0.0 %	0.0 %	0.0 %
14-10-1	0.0 %	0.0 %	0.0 %	0.0 %	0.0 %
12-10-1	0.0 %	0.0 %	0.0 %	0.0 %	0.0 %
12-8-1	1.56 %	1.56 %	1.56 %	1.56 %	1.56 %
10-8-1	2.81 %	3.70 %	2.50 %	1.25 %	3.70 %
10-6-1	1.56 %	1.56 %	1.56 %	1.56 %	1.56 %
8-6-1	3.28 %	3.75 %	2.81 %	2.81 %	3.75 %
8-4-1	6.71 %	5.31 %	5.61 %	6.25 %	9.68 %

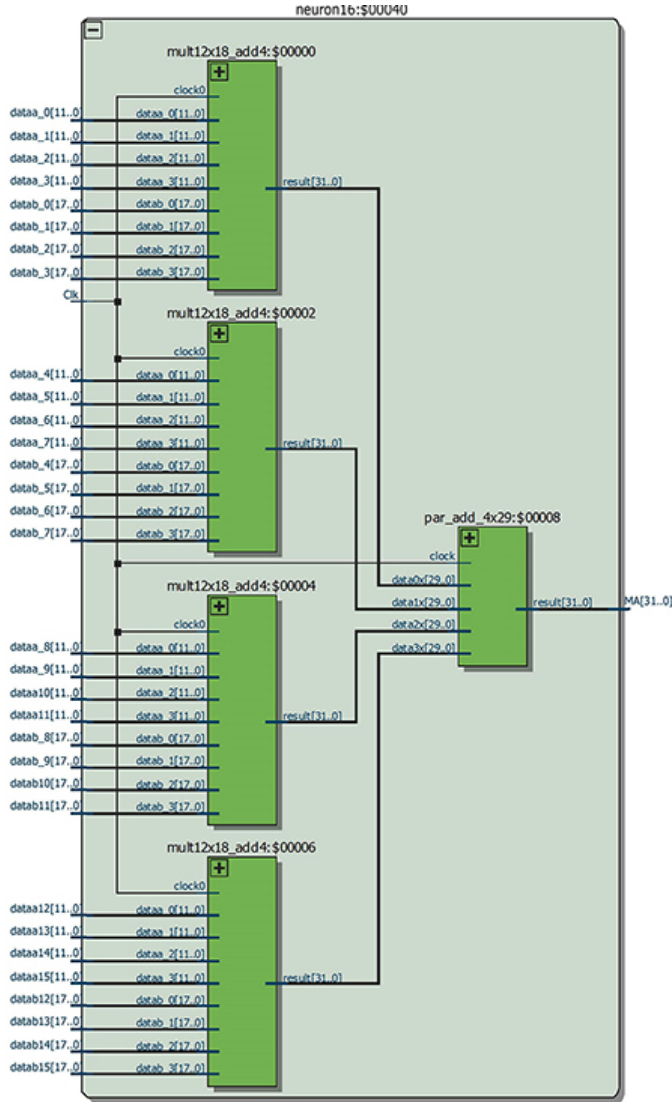


Fig. 8. An internal structure of an FPGA neuron.

Due to a limited amount of DSP blocks, we could use this network for a single PMT only. The Quartus[®] compiler allows a compilation with arbitrarily selected implementation of the multipliers: either in the DSP blocks or in logic elements only. An implementation of the multipliers in the Adaptive Logic Modules (ALMs) is much more resource-consuming (1247 ALMs instead of 107 ALMs + 8 DSP blocks), however such a selection allows an implementation of a more complicated network, which provides a similar performance (keeps approximately the same speed). The 3-channel 12-10-1 network needs 36 neurons (the 1st layer implemented in the DSP blocks) + 33 neurons implemented in 41151 ALMs (36.5% of 5CEFA9F3117).

The 12-10-1 network provides also a pretty fast convergence. A teaching process can be accomplished in several tens of epochs. Results from Tables II and III were obtained when networks were taught on selected patterns. However, teaching a bigger set of real Auger data for inclined showers (and others as references) gave rather surprising results that the network 12-8-1 provided better pattern recognition than 12-10-1.

IV. FPGA IMPLEMENTATION

A 16-input neuron for 14-bit data and 14-bit coefficients is shown in Fig. 8. A neuron output drives a neural transfer function - a tansig, which calculates a layer's output from its net input. It can be implemented as ROM in embedded FPGA memory. We selected a 14-bit input, 14-bit-output tansig implementation in RAM: a 3-port function with blocked writing left port to keep a reasonable compromise between a calculation accuracy and a memory size. Unfortunately, ROM: a 2-port failed. The same array of coefficients is used for two independent neuron transfer functions (Fig. 10).

The network was trained using 160 inclined and normal ADC traces (768 samples per trace). This gives 2×122880 patterns. For 160 inclined traces the network 12-8-1 recognized 139 inclined showers and only 27 patterns from a reference set (this rate should have been zero). However, taking into account the number of all patterns the rate of missing traces is 0.017% and the rate of wrongly recognized patterns 0.022%.

The fundamental algorithm for each neuron is as follows:

$$Neuron_{out} = \sum_{k=0}^{k-1} ADC_k \cdot C_{k,layer} + bias_{k,layer} \quad (1)$$

Neuron outputs are next scaled by a transfer function which is chosen to have a number of properties which either enhance or simplify the network containing the neuron. MATLAB offers the hyperbolic tangent sigmoid transfer (tansig) function. On-line calculation of the tansig in the FPGA is not necessary, it is enough to store in the ROM previously calculated values and to use the neuron output as addresses to the ROM. In order to keep a sufficient accuracy with a reasonable size of the embedded memory we used a 16384-word dual-port ROM with 14-bit output. For the network 12-8-1 we had to use 10 dual-port ROMs, which utilized 2240 kB of embedded memory (the output from the last layer was given directly to a comparator). Various parameterizations (Fig. 9) were tested for the best optimization. The best variant for the data used was with the scaling factor $sf = 1536$ which corresponds to the range of $(-5.33, \dots, +5.33)$ of the tansig argument (Fig. 9):

$$f_{index} = \frac{2}{1 + e^{-2 \cdot \frac{index - 8192}{sf}}} - 1. \quad (2)$$

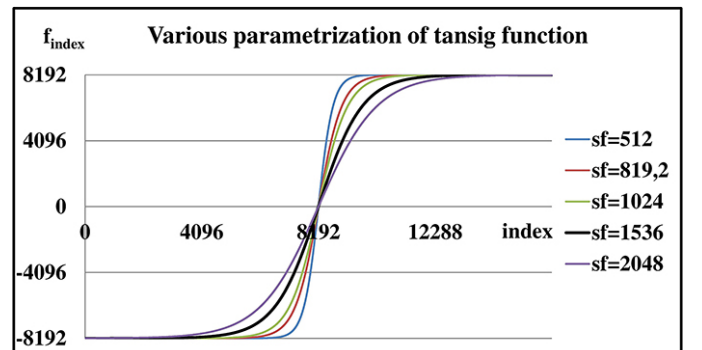


Fig. 9. Tested representations of the tansig function for the best optimization (Eq. 2).

ADC samples drive the 12-bit shift register whose output of sequential registers are connected to neuron inputs (Fig. 8). MATLAB provides a set of floating point coefficients obtained after a teaching process. In our practical implementation the FPGA uses the fixed point representation (FPR) to provide a fast enough registered performance and to utilize a reasonable amount of resources. There is no need to use floating point representation although Altera provides appropriate library procedures. For 12-bit input data at least 2 embedded DSP multipliers have to be used for a single multiplication in Eq. 1. The maximal width of the coefficients is 20-bit. However, we selected 18-bit coefficients to obtain a 32-bit width of neuron output (Fig. 8).

TABLE IV
SCALING, SUPPRESSION AND SHIFT FACTORS

Layer	SFS	SFL	SFX	SFB	SHP	SHN
1	2	131 072	8	524 288	-	6
2	4	32 768	8	32 768	14	1
3	2	32 768	2	32 768	13	1

All coefficients given by MATLAB have to be converted from a floating-point to fixed-point representation in two-component code. A simple conversion into two-component code is a multiplication of data by a fixed-point scaling factor (FPSF) and an addition of $2 \cdot \text{FPSF}$ for negative values. A condition is that the data must be in the $(-1.0, \dots, +1.0)$ range. Table IV shows all factors for scaling, suppressions and finally shifts of data. At first, coefficients (coeff and bias) calculated by MATLAB are suppressed (by factors SFS and SFX, respectively, to get a range $(-1.0, \dots, +1.0)$ (Eq. 3). Next, they are scaled by factors SFL and SFB, respectively (Eq. 4):

$$\text{coeff}_{k, \text{layer}, \text{fixed-point}} = \frac{\text{coeff}_{k, \text{layer}}}{\text{SFS}} * \text{SFL} \quad (3)$$

$$\text{bias}_{k, \text{layer}, \text{fixed-point}} = \frac{\text{bias}_{k, \text{layer}}}{\text{SFX}} * \text{SFB}. \quad (4)$$

The 32-bit signed output of the neuron (starting from the 2nd layer) is shifted right before a summation with bias due to very high values from the tansig transfer function (mostly either ~ 8192 or ~ 8191):

$$P = \left(\sum_{k=0}^{k-1} \text{ADC}_k \cdot C_{k, \text{layer}} \right) \gg \text{SHP}. \quad (5)$$

Addresses for the tansig function are additionally optimized to use the most sensitive function response region:

$$\text{address}_{k, \text{layer}} = (P \gg \text{SHN}) + 8192. \quad (6)$$

The highest bits from the neuron (Eq. 1) are neglected as irrelevant for a big argument of the tansig transfer function. Addresses are cropped to the range $< 0, \dots, 16383 >$.

In order to save some amount of memory we used Altera[®] library RAM: 3-port (as dual output ROM) with an initiation file, and blocked writing to the left port. The library function ROM: 2-port unfortunately failed. The same coefficient array is used for two independent addresses and gives two independent tansig coefficients. The RAM: 3-port saves twice

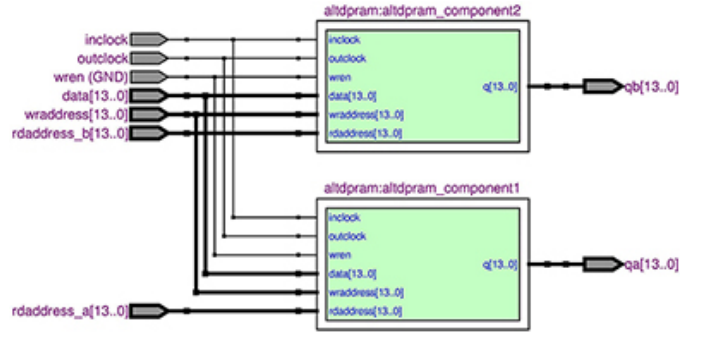


Fig. 10. 3-port RAM as a storage bank for tansig coefficients.

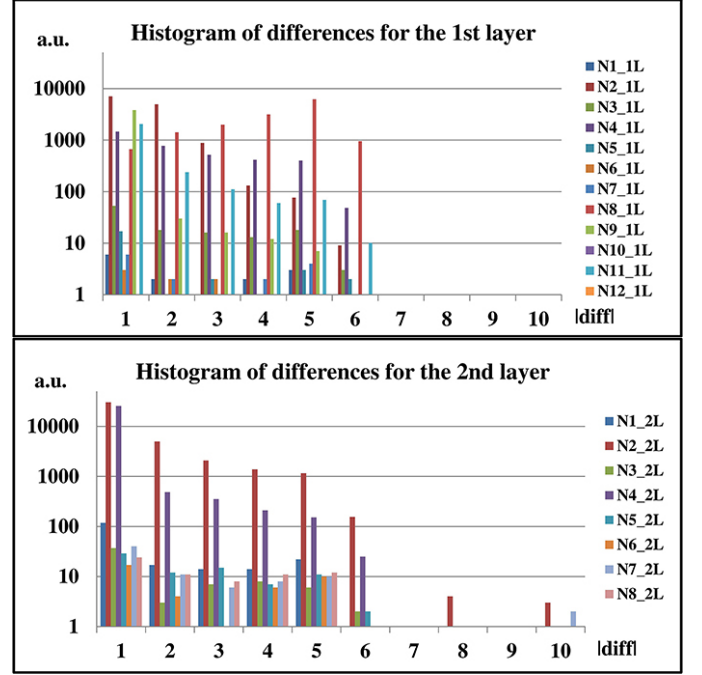


Fig. 11. Histogram of differences between the tansig integer output (from RAM: 3-PORT) and exact calculation for the 1st and 2nd layers.

embedded M9K memory blocks in comparison to a simple implementation of the ROM: 1-port library function.

An analysis of differences between the output data from neurons shows that differences reach a maximal value of only 1 ADC-unit. However, due to the relatively sharp slope of the tansig function in the central range, an error of 1 ADC-unit generates an output error of up to 6 ADC-units for the next (2nd) layer and even 10 ADC-units from the 2nd to the 3rd layer (Fig. 11). Nevertheless, the final error is negligible. A comparison of registered patterns for inclined showers (161/160) or spuriously recognized patterns for reference traces (39/160) shows that they are exactly the same as for the exact calculation (with double precision representation) and for the FPGA calculation in fixed-point representation with optimized bus and coefficients widths.

V. SIMULATIONS

The structure of the neuron network has been implemented in several FPGA families: Cyclone[®] III, Stratix[®] III and

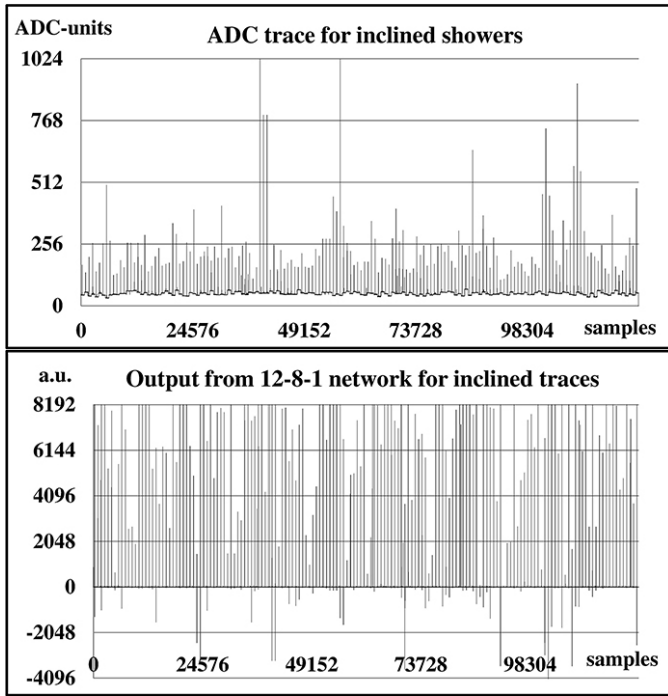


Fig. 12. ADC trace for positive-marked inclined showers (from 160 events) (upper graph) and corresponding output for 12-8-1 neural network (lower graph).

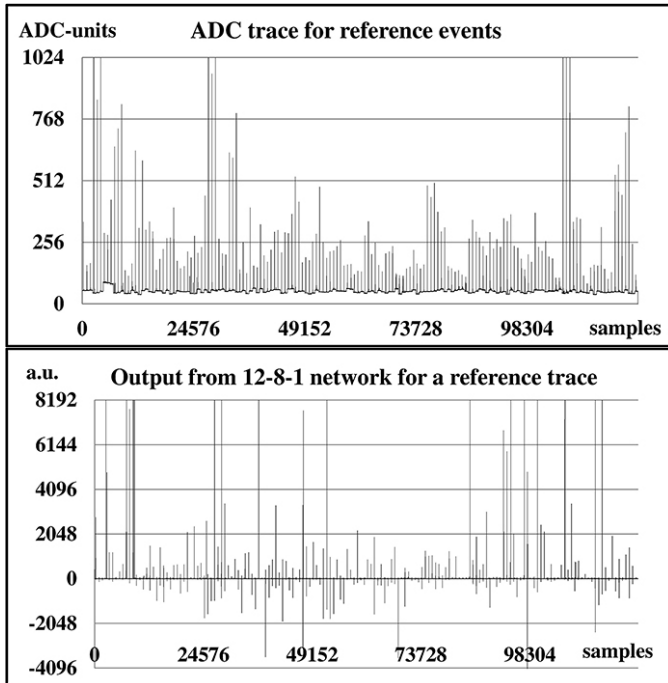


Fig. 13. ADC trace negative-marked reference showers (from 160 events) (upper graph) and corresponding output for 12-8-1 neural network.

Cyclone® V. The response of neural network on trained patterns was verified for 16-point inputs (taken from shift registers, where ADC data were permanently delayed sequentially) with fixed coefficients calculated in MATLAB. For the biggest FPGA from Cyclone® III family (EP3C120F780C7) the multipliers in the neuron from the last layer have to be

implemented in the logic cells due to a lack of DSP embedded blocks. This reduced the speed below our requirements. The middle-size FPGA EP3SL150F780C2 was a perfect chip for Quartus® simulation. We decided to make simulations using a relatively old tool: the Quartus® simulator as a much faster tool than the currently recommended ModelSim.

Figs. 12 and 13 show results of simulations for inclined (positive marker) and reference (negative marker) traces. For trained patterns the recognition is almost perfect. On 160 events with positive markers (totally 122 760 samples) 161 patterns were recognized by the 12-8-1 network (only a single false event - Fig. 12). On 160 reference events (with negative markers) 39 spurious events were registered, however, 12 of which had very high amplitude, which would have been also registered by the standard trigger.

Results of simulations confirm that the noise is perfectly rejected. On the output of the 3rd layer, the simple comparator was used instead of the tansig procedure (with an embedded memory).

VI. LABORATORY TESTS

The surface detector electronics is being improved from 10-bit 40 MSps to at least 12-bit 120/160 MSps ADCs. The University of Łódź has been developing the new Front-End Board based on the Altera® Cyclone® V 5CEFA9F31I7 and 8 channels supported by the ADS4249 (Texas Instr. 2-channel, 14-bits 250MSps ADCs) [25]. It can fully test the developing ANN also under real environmental conditions in the Argentinean pampas.

Before the field tests we were running laboratory tests based on the Altera development kit DK-DEV-5CEA7N driven via HSMC-ADC-BRIDGE from the ADS4249 Evaluation Module (EVM). The ADC on the EVM is driven from the two channel arbitrary function generator Tektronix AFG3252. The first channel generates patterns corresponding to the "old" showers (marker "+"), the second one generates reference traces (marker "-"). Channels are uncorrelated, they run with different frequencies and duty cycles (Fig. 14).

The FPGA trigger (either simple T1 or DCT based) freezes incoming traces and sends their output via the UART in NIOS to the PC. The virtual processor stores several hundred patterns in the RAM (both the developed FEB and the development kit contain a large enough external SDRAM). Thus, it starts the learning process with the algorithm extracted from the MATLAB package. Calculated coefficients are sequentially sent to the temporary D registers in the FPGA fast logic and are next simultaneously (in a single clock cycle) reloaded to the final registers driving the multipliers. Trigger rates for positively vs. negatively marked patterns agreed with our theoretical simulations.

VII. CONCLUSION

A huge amount of progress in electronics allows an introduction of new, much more powerful FPGAs and an implementation of much more sophisticated mathematical algorithms for real time processes. Neutrino physics is one of the discipline where new developments, in both hardware, and

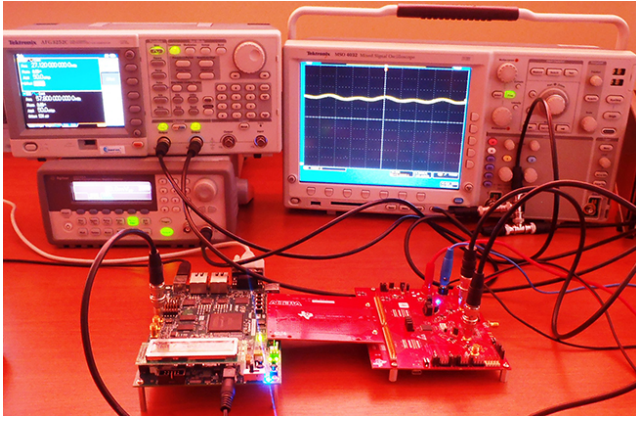


Fig. 14. Experimental setup with arbitrary pattern generators Tektronix AFG3252C and Agilent 33250A, Altera® Cyclone® V E development kit, Altera® HSMC-ADC-BRIDGE and Texas Instr. ADS4249EVM.

software, can significantly improve the efficiency of rare event detection. It is especially interesting where theories estimate neutrino fluxes over a very wide range.

The spectral trigger based on the Discrete Cosine Transform, offering a pattern recognition technique, has been already implemented in a test Front-End Board and tested in a test detector in Malargüe (Argentina). The new electronics developed according to the Auger-Beyond-2015 task in the Pierre Auger upgrade project allows an implementation of both DCT and ANN algorithms.

The Technical Board of the Pierre Auger Collaboration selected 8 surface detectors (a hexagon + twin in the center for an investigation of possible GPS jitter) in a north-west region of the SD array for tests of the new FEB on the Cyclone® V platform with 3-4 times higher sampling and 14-bit resolution with a cooperation of the SPMT and possibly other detectors. Simultaneously, the DCT triggers will be implemented in parallel with the standard ones to verify the detection of very inclined showers based on an on-line analysis of a shape of signals in the frequency domain.

This platform is appropriate also for tests of artificial neural networks. The biggest FPGA chip 5CEFA9F3117N in the new Front-End allows an implementation of two 12-8-1 networks with multipliers fully embedded in DSP blocks. Three PMTs require 3 networks. The FPGA is big enough to implement mixed DSP/fast logic multipliers for 3 networks.

We run CORSIKA [22] simulation for proton, iron, ν_μ and ν_τ primaries. Output data collected at 1450 m (the level of the Pierre Auger Observatory) was an input for OffLine [23] providing the ADC response in the WCDs. The obtained ADC traces were thus used to train the 12-8-1 neural network implemented already in the 5CEFA7F3117 FPGA on the Cyclone® V development kit. This FPGA is a smaller version of the chip being designed for the Front-End Board for the Auger-Beyond-2015 task. Preliminary results show that the 16-point ANN algorithm can detect neutrino events currently neglected by the standard Auger triggers and can support a recognition of neutrino-induced very inclined showers when ADC traces are relatively short and the muonic bump is better separated from the electromagnetic component.

ACKNOWLEDGMENT

The authors would like to thank the Pierre Auger Collaboration for an opportunity of using the CORSIKA and OffLine simulation packages.

REFERENCES

- [1] M. Nagano and A. A. Watson, "Observations and implications of the ultrahigh-energy cosmic rays", *Rev. of Modern Phys.*, vol. 72, no. 3, pp. 689-732, 2000.
- [2] F. Halzen and D. Hooper, "High-energy neutrino astronomy: the cosmic ray connection", *Rep. on Progress in Phys.*, vol. 65, no. 7, p. 1025, 2002.
- [3] J. K. Becker, "High-energy neutrinos in the context of multi-messenger astrophysics", *Phys. Reports*, vol. 458, no. 4-5, pp. 173246, 2008.
- [4] P. Bhattacharjee and G. Sigl, "Origin and propagation of extremely high-energy cosmic rays", *Phys. Reports*, vol. 327, no. 3-4, pp. 109-247, 2000.
- [5] J. Abraham et al. [Pierre Auger Collaboration], "Upper limit on the cosmic-ray photon fraction at EeV energies from the Pierre Auger Observatory", *Astropart. Phys.*, vol. 31, pp. 399-406, 2009.
- [6] K. Greisen, "End to the cosmic-ray spectrum?", *Phys. Rev. Lett.*, vol. 16, pp. 748-750, 1966.
- [7] G. T. Zatsepin and V. A. Kuzmin, "Upper limit of the spectrum of cosmic rays", *Pisma v Zhurnal Eksperimentalnoi i Teoreticheskoi Fiziki*, vol. 4, p. 114, 1966, English translation in: *JETP Letters*, vol. 4, p. 78, 1966.
- [8] [Hi-Res Fly's Eye Collaboration], "First Observation of the Greisen-Zatsepin-Kuzmin Suppression", *Phys. Rev. Lett.*, vol. 100, no. 10, article 101101, 5 pages, 2008.
- [9] [Pierre Auger Collaboration], "Properties and performance of the prototype instrument for the Pierre Auger Observatory", *Nucl. Instr. and Meth. ser. A*, vol. 523, no. 1-2, pp. 5095, 2004.
- [10] [Pierre Auger Collaboration], "Observation of the suppression of the flux of cosmic rays above $4 \cdot 10^{19}$ eV", *Physical Review Letters*, vol. 101, no. 6, article 061101, 7 pages, 2008.
- [11] K. Kotera, D. Allard, and A. V. Olinto, "Cosmogenic neutrinos: parameter space and detectability from PeV to ZeV", *JCAP*, vol. 2010, no. 10, article 013, 2010.
- [12] D. Seckel and T. Stanev, "Neutrinos: the key to ultrahigh energy cosmic rays", *Phys. Rev. Lett.*, vol. 95, no. 14, article 141101, 3 pages, 2005.
- [13] E. Zas, "Neutrino detection with inclined air showers", *New Journal of Phys.*, vol. 7, p. 130, 2005.
- [14] V. S. Berezinsky, A. Yu. Smirnov, "Cosmic neutrinos of ultrahigh energies and detection possibility", *Astrophys. and Space Sci.*, vol. 32, no. 2, pp. 461482, 1975.
- [15] [Pierre Auger Collaboration], "Ultrahigh Energy Neutrinos at the Pierre Auger Observatory", *Adv. in High Energy Phys.* vol. 2013, Article ID 708680, 18 pages.
- [16] K. S. Capelle, J. W. Cronin, G. Parente, and E. Zas, "On the detection of ultra high energy neutrinos with the Auger Observatory", *Astropart. Phys.*, vol. 8, no. 4, pp. 321328, 1998.
- [17] X. Bertou, P. Billoir, O. Deligny, C. Lachaud, and A. Letessier-Selvon, "Tau neutrinos in the Auger Observatory: a new window to UHECR sources", *Astropart. Phys.*, vol. 17, no. 2, pp. 183193, 2002.
- [18] [Pierre Auger Collaboration], "Upper limit on the diffuse flux of ultrahigh energy tau neutrinos from the Pierre Auger Observatory", *Phys. Rev. Lett.*, vol. 100, no. 21, article 211101, 2008.
- [19] Z. Szadkowski, "A spectral 1st level FPGA trigger for detection of very inclined showers based on a 16-point Discrete Cosine Transform for the Pierre Auger Observatory", *Nucl. Instr. Meth., ser. A*, vol. 606, pp. 330-343, July 2009.
- [20] Z. Szadkowski, "Trigger Board for the Auger Surface Detector with 100 MHz Sampling and Discrete Cosine Transform", *IEEE Trans. on Nucl. Science*, vol. 58, pp. 1692-1700, Aug. 2011.
- [21] Z. Szadkowski, "Optimization of the Detection of Very Inclined Showers Using a Spectral DCT Trigger in Arrays of Surface Detectors", *IEEE Trans. on Nucl. Science*, vol. 60, no. 5, pp. 3647-3653, Oct. 2013.
- [22] <https://web.ikp.kit.edu/corsika/>
- [23] S. Argiro et al., "The offline software framework of the Pierre Auger Observatory", *Nucl. Instrum. and Meth. ser. A*, vol. 580, Issue. 3, pp. 1485-1496, Oct. 2007.
- [24] [Pierre Auger Collaboration], "Trigger and aperture of the surface detector array of the Pierre Auger Observatory", *Nucl. Instr. Meth., ser. A*, vol. 613, pp. 29-39, Aug. 2010.
- [25] Z. Szadkowski, "Front-End Board with Cyclone® V as a Test High-Resolution Platform for the Auger_Beyond_2015 Front End Electronics, Contribution to the IEEE Real Time Conference, Nara (Japan), May 26-30, 2014.